Cell Reports

Enhancing pre-sexual and sexual differentiation of *Toxoplasma gondii* using retinal epithelial cells and intestinal organoids

Graphical abstract

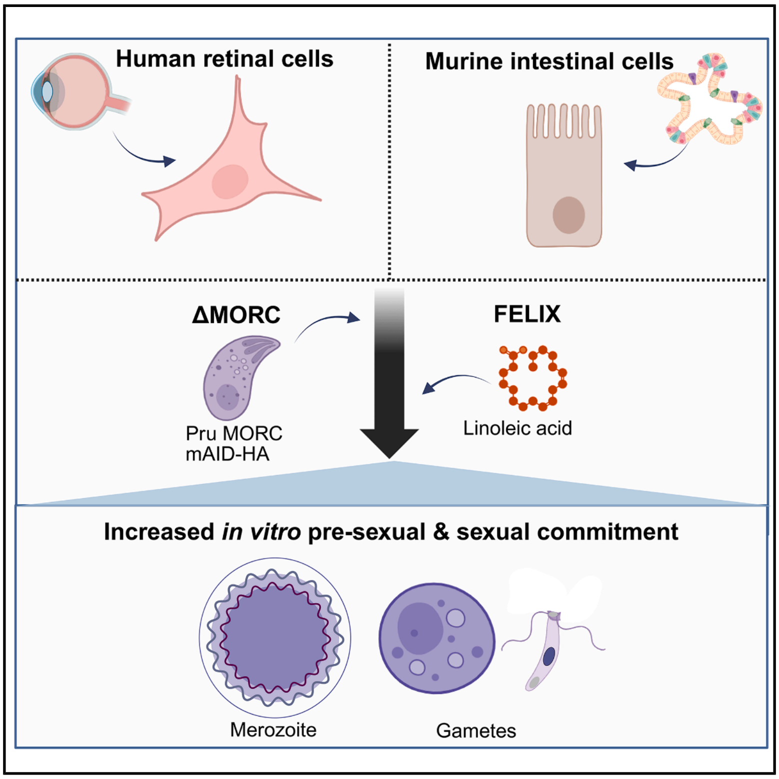

Authors

Saira Cancela, Florencia Sena,
Romina Pagotto, Martina Crispo,
Maria E. Francia, Mariela Bollati-Fogolín

Correspondence

mfrancia@pasteur.edu.uy (M.E.F.),
mbollati@pasteur.edu.uy (M.B.-F.)

In brief

Cancela, S. and Sena, F. et al. establish a non-feline *in vitro* model that enhances pre-sexual and sexual development of *T. gondii*. By integrating environmental conditions with genetic manipulation, they achieve synergistic stage conversion, providing an optimized platform to study the parasite's sexual cycle without relying on feline hosts.

Highlights

- Non-feline *in vitro* models support *T. gondii* pre-sexual and sexual stages
- Host cell type and parasite genetic variant combinations boost sexual differentiation output
- MORC depletion and FELIX medium synergize to promote stage conversion
- These models advance the study of *T. gondii* sexual development without feline hosts

Cancela et al., 2025, Cell Reports *44*, 116451
October 28, 2025
https://doi.org/10.1016/j.celrep.2025.116451

Cell Reports

CellPress
OPEN ACCESS

Report

Enhancing pre-sexual and sexual differentiation of *Toxoplasma gondii* using retinal epithelial cells and intestinal organoids

Saira Cancela,[1,2,7] Florencia Sena,[3,4,7] Romina Pagotto,[1] Martina Crispo,[2,5] Maria E. Francia,[3,6,8,*]
and Mariela Bollati-Fogolín[1,2,*]
[1]Cell Biology Unit, Institut Pasteur Montevideo, Montevideo, Uruguay
[2]Molecular, Cellular, and Animal Technology Program (ProTeMCA), Institut Pasteur Montevideo, Montevideo, Uruguay
[3]Laboratory of Apicomplexan Biology, Institut Pasteur Montevideo, Montevideo, Uruguay
[4]Laboratorio de Bioquímica, Departamento de Biología Vegetal, Facultad de Agronomía, Universidad de la República, Montevideo, Uruguay
[5]Laboratory Animal Biotechnology Unit, Institut Pasteur de Montevideo, Montevideo, Uruguay
[6]Unidad Académica de Parasitología y Micología, Facultad de Medicina, Universidad de la República, Montevideo, Uruguay
[7]These authors contributed equally
[8]Lead contact
*Correspondence: mfrancia@pasteur.edu.uy (M.E.F.), mbollati@pasteur.edu.uy (M.B.-F.)
https://doi.org/10.1016/j.celrep.2025.116451

SUMMARY

Toxoplasmosis, caused by *Toxoplasma gondii*, is a major global health concern due to its high prevalence, zoonotic transmission, and economic impact on livestock. The parasite's life cycle includes asexual, pre-sexual, and sexual stages, the latter responsible for oocyst shedding and genetic recombination. Understanding sexual differentiation is critical, but access has been limited because these stages occur only in the feline intestinal epithelium. Recent studies identify host metabolic cues and the microrchidia (MORC) protein complex as regulators of sexual commitment. We optimize *in vitro* approaches to enrich pre-sexual and sexual stages by combining a human retinal epithelial cell line and murine intestinal organoids with FELIX medium, which mimics feline intestinal biochemistry, and conditional MORC depletion. This system increases stage-specific gene expression and marker detection, demonstrating synergistic effects of host environment and genetic regulation. Our findings provide accessible models to study *T. gondii* sexual differentiation, with implications for controlling transmission and genetic diversity.

INTRODUCTION

Toxoplasma gondii is an obligate intracellular protozoan parasite of the phylum Apicomplexa and the causative agent of toxoplasmosis, a globally widespread zoonotic disease. Acute toxoplasmosis leads to reproductive failure and abortion, with significant economic consequences for the livestock industry.[1] In humans, acute infection can be asymptomatic or present mild flu-like symptoms, but in immunocompromised individuals or if acquired congenitally, it can cause severe encephalitis, blindness, or even death.[2] In addition, asymptomatic and largely undiagnosed acute infections invariably transition into chronic latent infections, at risk of reactivating upon immunosuppression. It is estimated that over one-third of the world's human population is chronically infected with *T. gondii*,[3,4] underscoring the epidemiological importance of understanding its life cycle and transmission.

The life cycle of *T. gondii* is complex, involving multiple developmental stages and highly adaptable transmission strategies. *T. gondii* can only complete its sexual cycle in the intestines of felids, its definitive hosts. Here, it differentiates into gametes, which can recombine, generating genetic diversity and producing oocysts that are shed into the environment.[5] A single infected cat can release hundreds of millions of oocysts, which remain infectious for over a year.[6]

Despite its major role in environmental dissemination and genetic diversity, the sexual cycle of *T. gondii* remains superficially understood due to its difficult *in vitro* access. Historically, *T. gondii* infection studies have relied on murine *in vivo* models or immortalized cell lines such as human foreskin fibroblast (HFF), monkey kidney epithelial cells (Vero), or human colorectal adenocarcinoma cells (Caco-2). While these models have been instrumental in studying the parasite's asexual replication, they fail to support complete pre-sexual and sexual parasite differentiation. Recent advances in the three-dimensional (3D) organoid[7] technology have provided more physiologically relevant models to study enteric host-pathogen interactions. Murine, farm animals, and human intestinal organoids have been successfully infected with *T. gondii*,[8–10] enabling studies of early infection dynamics and parasite-host interactions. However, these models have not yet supported the complete sexual cycle, likely due to the absence of feline-specific metabolic and molecular factors necessary for gamete formation and oocyst development.[12]

Foundational *in vivo* studies uncovered the merozoite preceding the formation of macro and microgametes, whose recombination culminates in fertilization and oocyst formation.[13–15] However, these have until recently been inaccessible *in vitro*. Recent breakthroughs in understanding the factors governing *T. gondii* sexual differentiation have opened new research avenues. Specifically, the biochemical signature that led felines to be selected as the definitive host by this parasite has been identified; an accumulation of linoleic acid in feline intestines resulting from the lack of delta-6-desaturase activity was shown to be essential for the initiation of *T. gondii* gametogenesis.[16] Additionally, the microrchidia (MORC) protein complex has been identified as a master regulator that, by coupling its activity with that of a histone deacetylase, represses the expression of sexual-stage genes. Upon TgMORC (*T. gondii* MORC)'s conditional silencing, sexual stages are induced.[17] These findings provide a unique opportunity to optimize *in vitro* models that bypass the need for felines while enabling the study of *T. gondii* sexual differentiation under controlled conditions.

Here, we aim to develop innovative *in vitro* models designed to mimic the feline intestinal environment and promote *T. gondii* sexual differentiation. We combine the use of a media composition mimicking the biochemistry of the feline intestinal environment, which we have termed FELIX (felid-environment like with linoleic acid excess), intestinal organoid-derived monolayers (ODMs), and a human retinal epithelial cell line while simultaneously depleting TgMORC, to recreate key metabolic and molecular conditions required for the parasite's sexual commitment. By leveraging these systems, we achieve a synergistic enrichment of pre-sexual and sexual stages, as demonstrated by the upregulation of stage-specific genes and the localization of pre-sexual and sexual-stage markers using qPCR and immunofluorescence assays.

RESULTS

Host cell type, culture format, and FELIX media differentially influence *T. gondii* differentiation and infection efficiency

We first evaluated the relative contributions of a three-component system to induce tachyzoite differentiation into pre-sexual and sexual stages of *T. gondii*. We combined cellular types and culture formats, with the PruΔku80 MORC-mAID-Tir-HA strain,[17] and the use of culture media, mimicking the intestinal felid environment described first by Martorelli and colleagues.[16] The PruΔku80 MORC–mAID–Tir–HA strain allows for selective and conditional MORC depletion. Depletion results in marked transcriptional changes that shift parasites from asexual proliferation to sexual differentiation.[17] To evaluate the host's contribution to *T. gondii* differentiation stages, we selected representative cell lines derived from different organs for which *T. gondii* exhibits physiological interactions, such as the intestine, retina, and the central nervous system. The kidney-derived Vero cells were used as controls. In addition, we compared the output of the 2D and 3D model systems. Finally, we combined the aforementioned variations with FELIX media, a growth medium mimicking the felid intestinal environment as described in STAR Methods.

First, we assayed the infection of Vero, hRPE, Caco-2, and NSC-34 cells with the PruΔku80 MORC–mAID–Tir-HA strain. We monitored parasite infections through the detection of bradyzoites by IFA using an anti-CC2 antibody[18] (Figure 1A). We quantified the bradyzoites population over the total amount of parasites with or without FELIX in the different cell lines, either in the amount of cysts (Figure 1B) or in the total number of bradyzoites per cyst (Figure 1C). The total number of bradyzoite-containing vacuoles did not show significant differences across the different cell lines; however, the number of bradyzoites per cyst varied significantly between cell lines. Infection of hRPE cells resulted in the highest number of bradyzoites formed, reaching up to 80 bradyzoites per vacuole when MORC depletion was induced in FELIX media as compared to 33 in Vero and four in Caco-2 and NSC-34 cells. As bradyzoite formation is thought to precede pre-sexual and sexual differentiation, we reckon that continuing with this cell line for further experiments could promote differentiation more efficiently.

To pursue *T. gondii* infections in murine intestinal organoids, we first assessed the parasite's ability to invade and replicate within the intestinal epithelium in both 2D and 3D culture systems. Immunofluorescence analysis of tachyzoite surface antigen SAG1 confirmed intracellular parasite localization and active parasite replication 24 h post-infection in whole organoids and ODMs (Figure 1D). Lysozyme staining revealed the presence of specialized epithelial cells, while phalloidin and DAPI staining highlighted epithelial structure and nuclear distribution within infected cells. Although *T. gondii* was able to invade and replicate in both systems, quantification of tachyzoites suggested a higher infection efficiency in the 2D monolayer compared to the 3D organoid culture (Figure 1E). Additionally, we determined that FELIX compounds did not induce detectable cytotoxicity (Figure S3).

FELIX treated human retinal cells induce pre-sexual and sexual stages of *T. gondii in vitro*

We next examined the experimental conditions under which the gene expression of specific markers of asexual (*SAG1* and *BAG1*), pre-sexual (*GRA81* and *GRA11b*), and sexual (*PF16*, *IFT122*, and *AO2*) stages of parasite differentiation was optimally induced. Using hRPE cells, *T. gondii* was cultured under different experimental conditions: control condition (−IAA [indole-3-acetic acid] and −FELIX), MORC depletion only (+IAA, − FELIX), FELIX only (−IAA and + FELIX), and dual-treatment (+IAA and + FELIX). We found that the assayed conditions differentially affected gene expression both in 2D cell line culture and in the intestinal ODMs (Figures 2 and 4). First, consistent with what was previously reported in HFFs, the addition of IAA to induce MORC depletion, alone, showed a significant increase in the merozoite marker *GRA81* and the macrogamete marker *AO2*. In hRPE cells, gene expression of these markers was induced 5- and 40-fold, respectively. Surprisingly, FELIX media alone induced an increase in gene expression of the microgamete *IFT122* marker by 40-fold. Finally, the combination of MORC depletion and FELIX media showed the highest expression levels for all markers, revealing a synergic interaction between both conditions. We observed a statistically significant increase in the relative expression of the asexual stage marker *BAG1* by

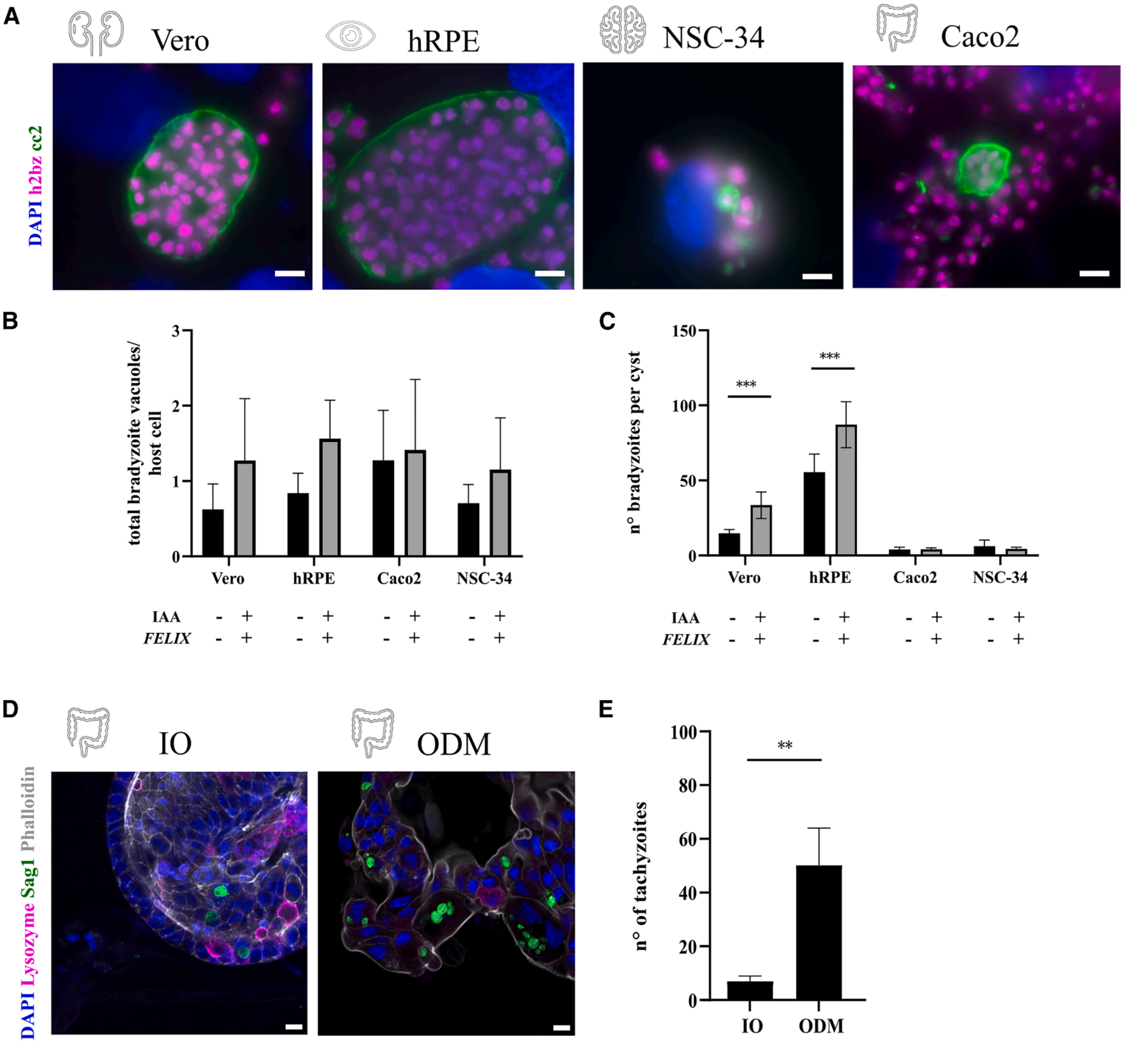

Figure 1. hRPE cells sustain bradyzoite conversion more efficiently than other cell types, and *T. gondii* infects both 2D and 3D intestinal organoids

(A) Host cells infected with the PruΔku80 MORC–mAID–Tir-HA strain under IAA for 7 days. Staining corresponds to parasite histone h2bz (magenta), bradyzoite cell wall cc2 (green), and nuclei with DAPI (blue). Scale bar represents 10 μm.

(B and C) Host cells infected with the PruΔku80 MORC–mAID–Tir-HA strain grew with or without FELIX media complemented with or without IAA for 7 days. The total number of bradyzoite vacuoles anti-cc2-positive was counted and normalized by total host cell nuclei (DAPI+) (B), and the number of bradyzoites per cyst by the detection of anti-cc2 signal in relation to total nuclei by h2bz was plotted (C). The asterisks represent statistically significant differences by Student's t test (***$p < 0.001$, $n = 5$).

(D) Intestinal organoids (IOs) and ODMs infected with the PruΔku80 strain of moderate virulence for 24 h. Staining corresponds to lysozyme (magenta), tachyzoite membrane protein Sag1 (green), phalloidin (gray), and nuclei with DAPI (blue). Scale bar represents 10 μm.

(E) Number of tachyzoites by the detection of anti-Sag1 signal in IO and ODM. The asterisks represent statistically significant differences by Student's t test (***$p < 0.001$. $n \approx 10$).

Scale bars, 10 μm. The values represent the mean, and the bars are the standard error of the mean (SEM).

5-fold during the depletion of MORC and the incubation in the FELIX media with respect to the control (p value < 0.001 and 0.0001) (Figure 2A). The pre-sexual marker *GRA11b* showed the highest relative expression level changes, with a 150-fold increase. The marker *GRA81* also increased by approximately 13-fold (Figure 2B). Finally, we determined that female (*AO2)* and male (*PF16*) gamete markers increased by approximately 150-fold and 50-fold, respectively (Figure 2C).

To assess whether the observable gene expression changes correlated with the increased generation of each stage, we monitored the different parasite stages by IFA (Figure 3A). For this, we infected hRPE cells with tachyzoites under the same experimental conditions described above and assayed the expression of stage-specific proteins. We detected bradyzoite cysts by staining with anti-cc2 antibody, the dense granule protein of merozoites by staining with anti-GRA80 antibody,[19] and the

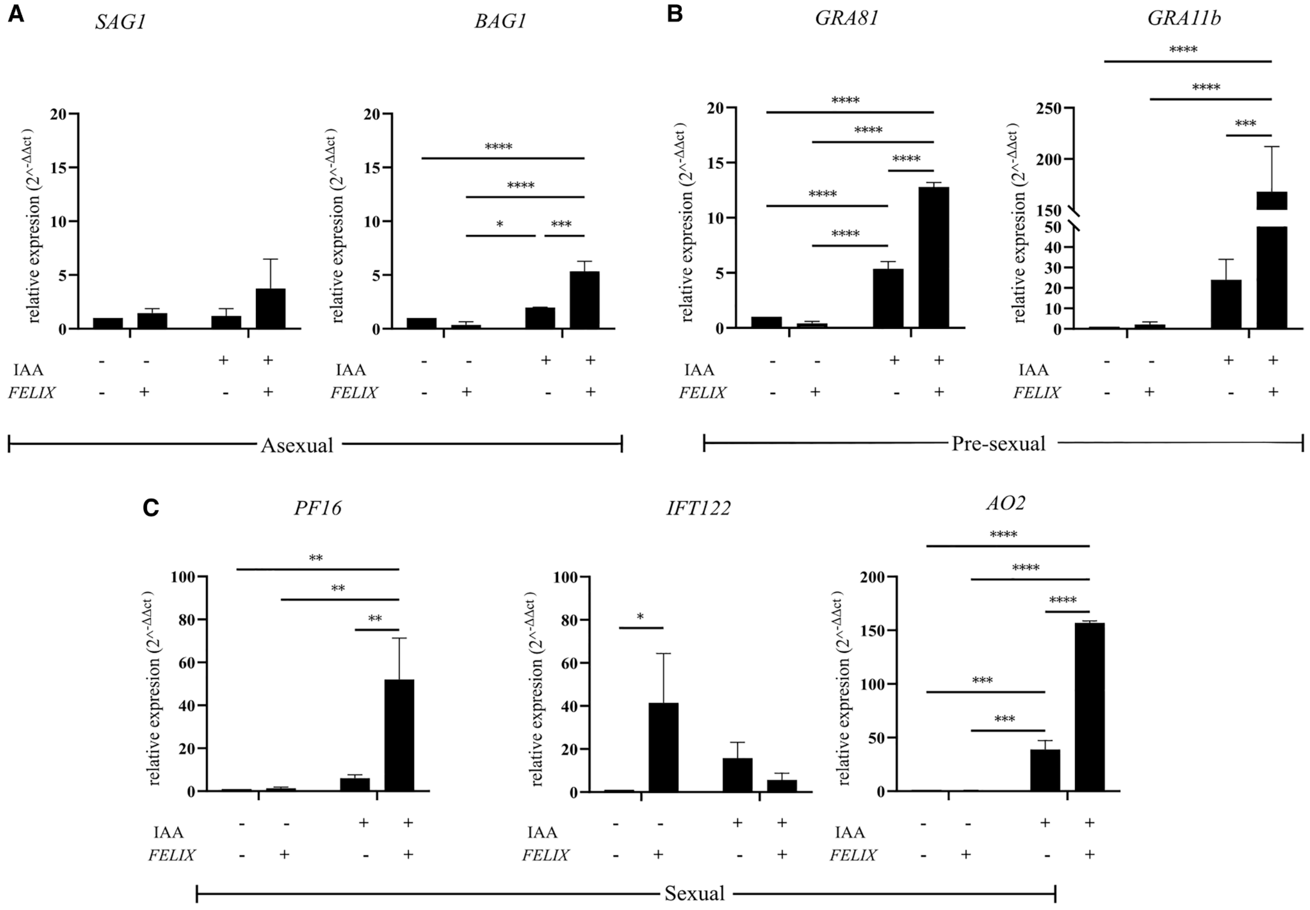

Figure 2. Pre-sexual and sexual stage genes' expression is significantly increased in *T. gondii* cultured in hRPE cells when cultured in *FELIX* and MORC is depleted

Relative gene expression ($2^{-\Delta\Delta Ct}$) of tachyzoite (*SAG1*), bradyzoite (*BAG1*) (A), merozoite (*GRA81* and *GRA11b*) (B), and gametes markers (*PF16*, *IFT122*, and *AO2*) (C) in PruΔku80 MORC–mAID–Tir-HA parasites cultured in hRPE cells with or without IAA and/or with or without the FELIX media.

The values of gene expression represent the mean, and the bars are the SEM. Asterisks indicate statistically significant differences by ANOVA test (*$p < 0.05$, **$p < 0.01$, ***$p < 0.001$, and ****$p < 0.0001$. $n = 3$).

copper amine oxidase protein from female gametes by staining with the anti-AO2 antibody.[16] Quantifications of different stage occurrences revealed that bradyzoites were about 10% enriched in hRPE cells under simultaneous MORC depletion (+IAA condition) and FELIX media treatment, compared to that of MORC depletion alone. However, this difference was not statistically significant. In contrast, GRA11b expressing merozoites represented around 20% of the culture under either MORC depletion or FELIX media treatment, while the percentage of merozoites largely increased, reaching over 50% under dual treatment (Figures 3B and 3C). Notably, while we were able to seldom detect AO2 signals, suggesting the presence of *in vitro* macrogametes (Figure 3A), their rare occurrence precluded their precise quantification.

FELIX treated murine intestinal ODMs induce pre-sexual and sexual stages of *T. gondii in vitro*

To assess whether a more physiologically relevant environment could better support *T. gondii*'s sexual development, the individual and added contributions of MORC depletion and FELIX media were evaluated using intestinal epithelial cells as host. In this model, ODMs were used, and similar transcriptional changes spanning asexual, pre-sexual, and sexual markers were evaluated.

As observed in the monolayers of hRPE, asexual stage markers showed a moderate increase in expression levels compared to non-induced controls in ODMs. The expression of the tachyzoite marker *SAG1* remained similar under FELIX but increased ~2-fold upon MORC depletion alone, reaching a statistically significant difference of ~3-fold only under dual treatment (Figure 4A, left). Similarly, the expression of the bradyzoite marker *BAG1* increased ~2.5-fold upon MORC depletion alone, and ~4-fold under dual-treatment, but no significant differences were observed in the expression levels under FELIX only (Figure 4A, right). These results indicate a general rise in asexual gene expression in ODMs, particularly in response to the combined treatment of FELIX and MORC depletion.

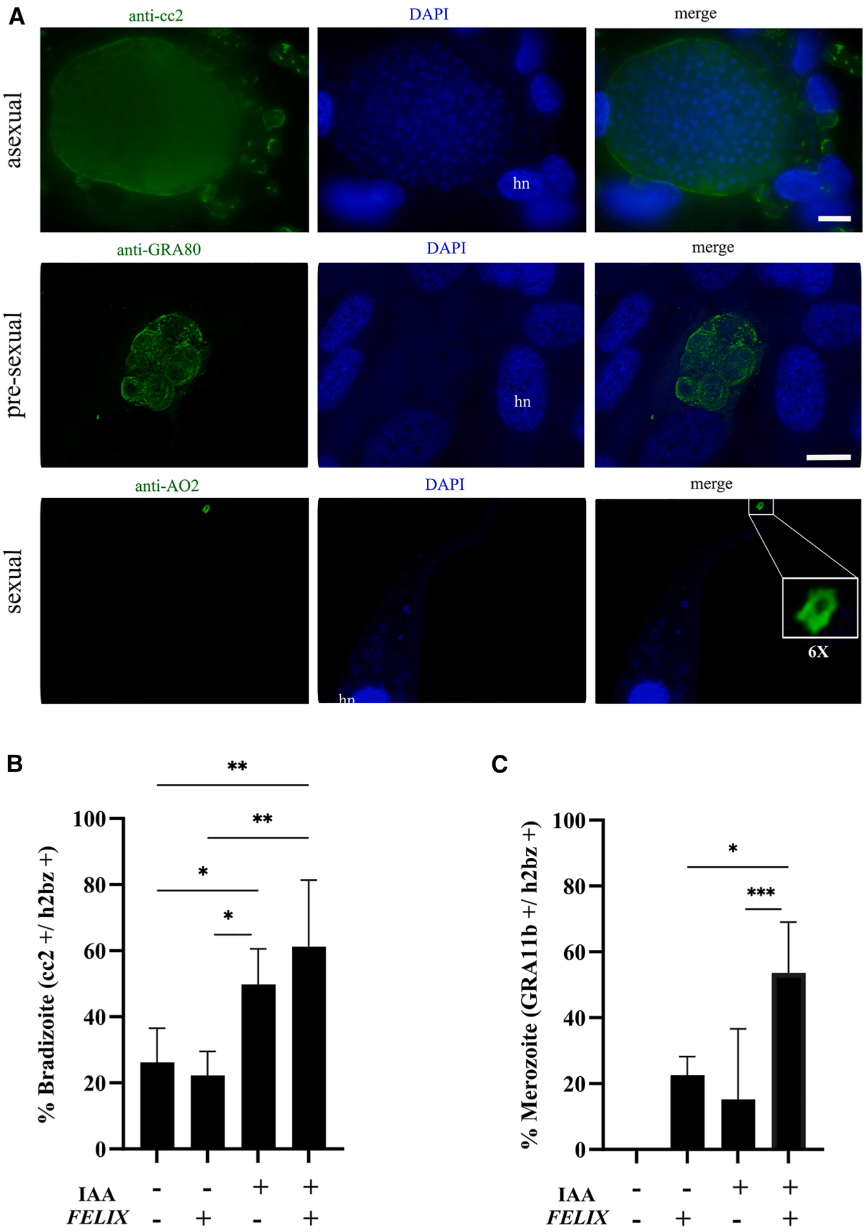

Figure 3. *T. gondii* pre-sexual and sexual forms are detected at higher levels in hRPE cells when cultured in *FELIX*, and MORC is depleted

(A) Immunofluorescence assay showing markers of different parasite stages were used: anti-cc2 (green) to the asexual stage of bradyzoite, anti-GRA80 (green) to the pre-sexual stage of merozoite, and anti-AO2 (green) to the sexual stage of macrogamete. Host and parasite nuclei were stained with DAPI (blue). hn, host nucleus. Scale bars, 10 μm.

(B) Bradizoite and (C) merozoite quantification from IFAs. The percentage of either bradizoite or merozoite is represented as the mean of cc2- or GRA11b-positive signal in relation to the total parasite marked with h2bz. The values represent the mean, and the bars are the SEM. Asterisks indicate statistically significant differences by Student's t test (*$p < 0.05$, **$p < 0.01$, and ***$p < 0.001$. $n \geq 5$).

Interestingly, the pre-sexual merozoite markers *GRA81* and *GRA11b* were robustly upregulated. *GRA81* expression increased ~2-fold with FELIX and ~10-fold upon MORC depletion alone, respectively, but displayed a marked ~25-fold increase under dual treatment (Figure 4B, left). Notably, *GRA11b* showed the most significant induction among all genes analyzed, with an approximately 60-fold increase under MORC depletion alone and a ~120-fold upregulation under dual treatment (Figure 4B, right). These results highlight a strong synergistic effect of FELIX and MORC depletion in promoting the pre-sexual transcriptional merozoite program. Finally, sexual stage markers followed a similar trend. The microgamete marker, *PF16*, was the most significantly upregulated with ~30-fold under MORC depletion alone; it yielded a ~35-fold increase upon dual-treatment, again suggesting an additive effect (Figure 4C, left). The intraflagellar transport protein *IFT122* gene expression displayed a ~2.5-fold increase under dual-treatment (Figure 4C, middle). The macrogamete marker *AO2* gene expression increased ~2.5-fold upon MORC depletion and ~3.5-fold under the dual treatment (Figure 4C, right). Altogether, these observations suggest that FELIX alone can support slight changes in the expression level of certain genes, while its concomitant MORC depletion is required for synergistic activation of the transcriptional programs required for *T. gondii*'s differentiation, with particularly strong effects on pre-sexual commitment.

To assess whether the transcriptional activation observed by qPCR correlated with stage-specific parasite development, we performed IFAs in *T. gondii*-infected murine intestinal ODMs, cultured under the same experimental conditions used to assess gene expression changes. Under concomitant FELIX and MORC depletion, we evaluated the expression of stage-specific proteins. Presence of asexual forms was confirmed by the detection of the bradyzoite cysts protein CC2 (Figure 5A). In line with the transcriptional data, pre-sexual merozoites were detected in FELIX-treated and induced cultures by staining with the anti-GRA11b antibody. GRA11b+ vacuoles co-localized with the nuclear H2 histone variant H2Bz, confirming their merozoite identity (Figure 5A). Consistent with the qPCR results, which showed increased relative expression of GRA11b in the FELIX-treated and MORC depletion treatments compared to individual treatments and control, quantification of immunofluorescence images revealed

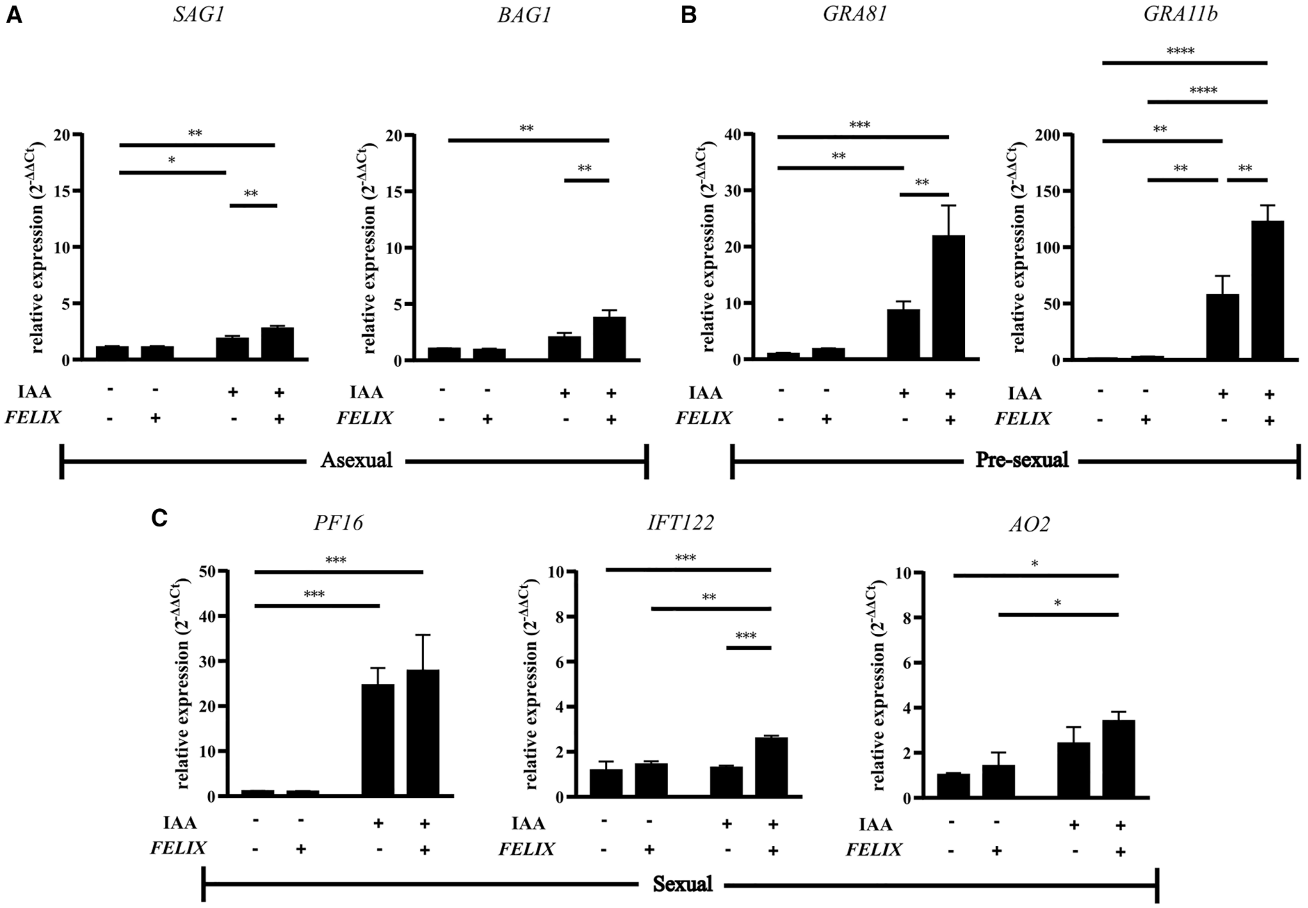

Figure 4. *T. gondii* pre-sexual and sexual stage genes' expression is significantly increased in ODMs treated with *FELIX* and upon MORC depletion

Relative gene expression ($2^{-\Delta\Delta Ct}$) of tachyzoite (*SAG1*), bradyzoite (*BAG1*) (A), merozoite (*GRA81* and *GRA11b*) (B), and gametes markers (*PF16*, *IFT122*, and *AO2*) (C) in *T. gondii* PruΔku80 MORC–mAID–Tir-HA parasites cultured in murine intestinal ODMs with or without IAA and/or with or without FELIX media. The values of gene expression represent the mean, and the bars are the SEM. Asterisks indicate statistically significant differences by ANOVA test (*$p < 0.05$, **$p < 0.01$, ***$p < 0.001$, and ****$p < 0.0001$. $n = 3$).

a significant increase in GRA11b+ parasites (≈60%) under dual treatment, compared to individual treatments (Figure 5B). These results reinforce the synergistic role of these stimuli in inducing pre-sexual differentiation in *T. gondii*.

We also assessed the presence of the macrogamete marker AO2. Conspicuously, although this marker was significantly upregulated at the mRNA level under dual treatment conditions, it was not readily observable by immunofluorescence. This discrepancy may be a consequence of low protein abundance, differences in detection sensitivity between qPCR and IFA, or a delay in protein expression following gene transcription.

Altogether, our findings support the notion that FELIX and MORC depletion work together to promote *T. gondii* differentiation into pre-sexual stages, as evidenced at both the transcript and protein levels. This synergistic effect triggers the changes in transcription levels that qualitatively resemble more closely to the *in vivo* expression patterns along the asexual to pre-sexual differentiation axis than MORC depletion alone (Figure S4).

DISCUSSION

In recent years, technical breakthroughs have shed tremendously needed light onto the regulatory elements that govern *T. gondii*'s sexual differentiation. Prior to these studies, sexual structures had only been observed by electron microscopy in studies from the 70s, but the regulatory elements triggering the formation of such structures were unknown.[14,20] Transcriptomic data of pre-sexual and sexual forms, transcriptional regulators, as well as environmental cues were uncovered.[17,19,21–25] Here, we capitalized on previously established findings to assess whether combining them through the use of specific cell types, biochemical manipulation of the environment, and parasite genetic manipulation could yield an *in vitro* system that optimizes the transition of *T. gondii* from asexual to pre-sexual and sexual stages. In addition, we incorporated two physiologically relevant systems: retina epithelial cells, an environment that we show naturally promotes the parasite's transition to the bradyzoite stage, and an intestinal organoid model. We showed that both

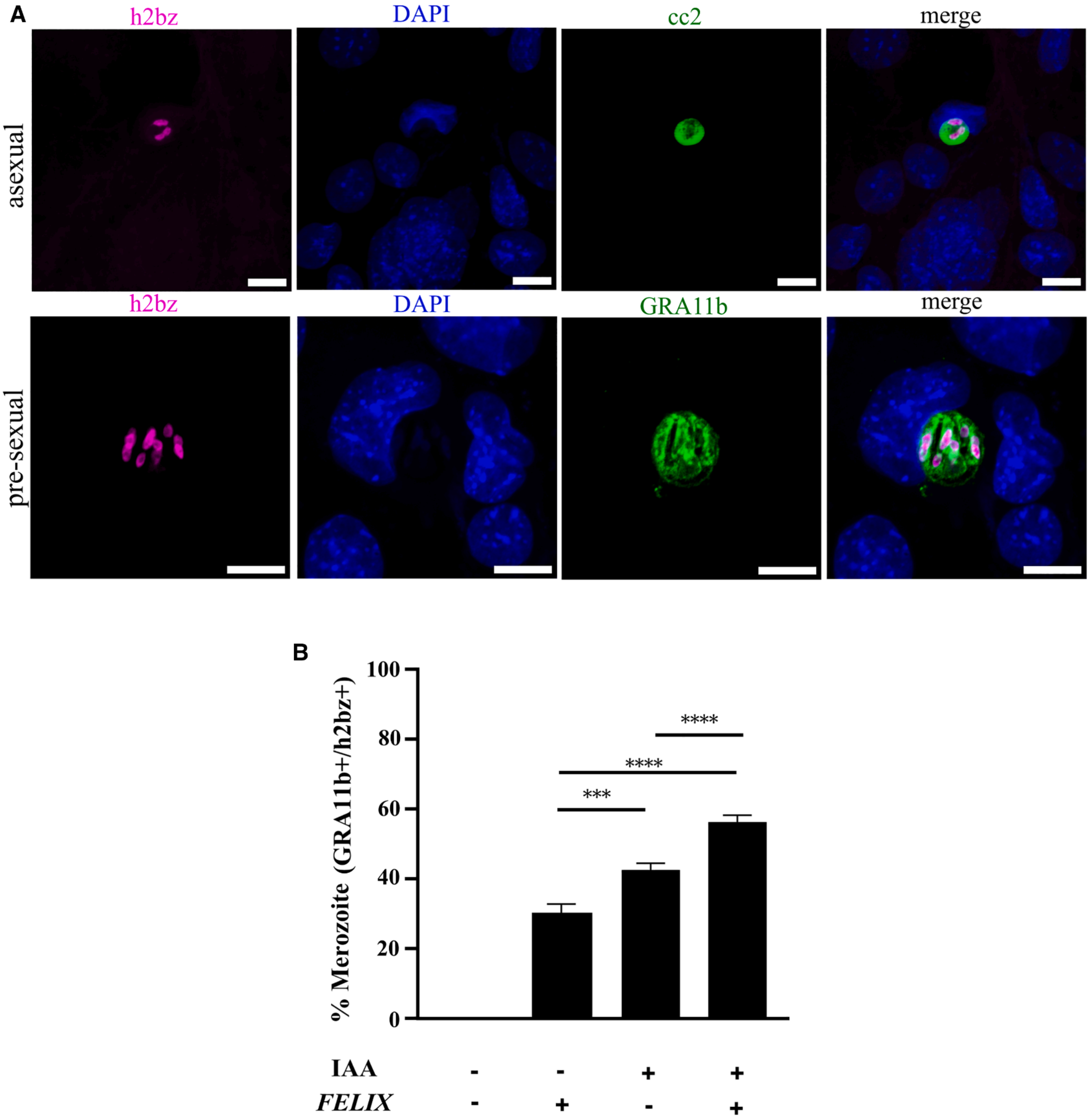

Figure 5. *T. gondii* pre-sexual and sexual forms are detected at higher levels in intestinal ODMs treated with FELIX and upon MORC depletion

Markers of different parasite stages were used: (A) anti-cc2 (green) for the asexual bradyzoite stage and anti-GRA11b (green) for the pre-sexual merozoite stage. Nuclei were stained with DAPI (blue), and parasite nuclei were stained with anti-h2bz (magenta). Scale bars, 10 μm.

(B) Merozoites quantification by anti-GRA11b+ signal in relation to total nuclei h2bz+. The values represent the mean, and the bars are the SEM. Asterisks indicate statistically significant differences by ANOVA test (*$p < 0.05$, **$p < 0.01$, ***$p < 0.001$, **** and $p < 0.0001$. $n = 50$).

the retinal cell lines and epithelial monolayers derived from murine intestinal organoids supported the differentiation of tachyzoites to pre-sexual and sexual stages when FELIX media are used concomitantly with MORC depletion.

The presence of excess linoleic acid, which is uniquely abundant in feline intestines, was already reported in the 70s.[26,27] Foundational studies demonstrated that *T. gondii* undergoes stage conversion when exposed to metabolic stressors, particularly lipid imbalances determined by linoleic acid excess.[21] However, the use of exogenous linoleic acid has been reported to be parasiticidal to *T. gondii* tachyzoites in a dose-, duration-, and cell-dependent manner. Interestingly, linoleic acid is much less parasiticidal in Caco-2 than in HFF cells.[28] Under our experimental conditions, the excess of linoleic acid did not affect the viability of either parasites or host cells.

Additionally, retinoic acid has been implicated in modulating host-pathogen interactions of gastrointestinal parasites and immune responses.[29] While its specific role in *T. gondii* sexual differentiation remains unclear, its presence in the feline intestine suggests it may act synergistically with linoleic acid to create an environment conducive to gametocytogenesis. It is worth noting that retinoic acid was included in our hRPE assays, as these assays implied first inducing transition to the bradyzoite stage for 7 days, to then deplete MORC. This reagent was not included in our ODM assays, as infections were done more acutely, for a maximum of 48 h, due to the inherent limitations of long-term organoid culture. Further studies should aim to disentangle the individual contributions of linoleic and retinoic acid in differentiation.

In this study, we explored several cell types associated with natural stage-specific transitions of *T. gondii*, including intestinal cells (Caco-2) and nervous system cells (NSC-34 and hRPE). We found that human retinal pigment epithelial cells and 2D intestine monolayers more effectively support sexual differentiation of *T. gondii*. Retinal pigment epithelial cells have historically served as a model for ocular toxoplasmosis and parasite transmigration.[30,31] Infection of RPE cells by *T. gondii* disrupts epithelial barrier function, promotes parasite dissemination,[32–34] and alters the secretion of growth factors, increasing infection susceptibility.[35–37] Recently, human retinal organoids were successfully infected with *T. gondii* tachyzoites, and live parasites were detected from the margin to the entire organoid over a week post infection.[38] Here, we show that hRPE cells supported highly efficient bradyzoite formation, and this coincided with enhanced differentiation into pre-sexual and sexual forms. This correlation suggests a potential link between bradyzoite formation and sexual commitment under specific conditions, highlighting a potential cell-type-specific influence on developmental trajectories. The upstream "natural" pathways that precede the natural transition to pre-sexual stages remain controversial. Felid infections are initiated either by ingestion of sporozoite-containing oocysts or ingestion of tissue cysts filled with bradyzoites. After ingestion of the latter, bradyzoite release is facilitated by gastric passage at the small intestine, from which infection of the intestinal epithelium onsets.[39] A key unanswered question remains whether the transition to sexual stages necessarily proceeds through the bradyzoite stage or whether it can directly initiate from tachyzoites. Whether bradyzoite formation primes sexual development is still to be shown. It has been demonstrated that deletion of two ApiAP2 transcription factors enables direct conversion from tachyzoites to pre-sexual forms *in vitro*,[19,22] bypassing bradyzoite formation altogether. Though these mutants are unable to fully differentiate into sexual stages, it is worth considering that multiple initiating pathways might support sexual differentiation.

Nonetheless, our results show that with the striking exception of *IFT22* in hRPE cells, parasite genetic manipulation was required for stage-specific induction of transcriptional changes. These results demonstrate that the environmental cues identified alone are not sufficient to induce the expression of pre-sexual and sexual stage markers *in vitro*, even in intestinal organoids, thus suggesting that additional environmental cues are essential to exogenously trigger differentiation into these stages.

Our results align with the demonstrated role of MORC. MORC is part of a chromatin-remodeling complex, which negatively regulates *T. gondii* sexual differentiation. MORC depletion leads to the upregulation of multiple sexual stage markers, including genes associated with gametocyte development and flagellar assembly.[17] In our system, the combined effect of FELIX and MORC depletion resulted in a more robust differentiation response, suggesting that while MORC depletion facilitates the intrinsic transcriptional shift required for pre-sexual and sexual commitment, metabolic external signals are also integrated in the response network. Specifically, the presence of a metabolically permissive environment—such as one rich in linoleic acid, as found in felids—appears to enhance the response, pointing to a possible synergistic interplay between parasite-intrinsic epigenetic regulation and extrinsic host cues. This raises important questions about the upstream and downstream regulators of MORC activity and how its activity is modulated in response to host signals. It is plausible that host lipid environments influence parasite metabolism and chromatin state, either through direct metabolite availability (e.g., acetyl-CoA or fatty acid-derived signaling lipids) or indirectly through signaling pathways yet to be defined. Additionally, the extent to which MORC repression must be relieved to achieve full gametogenesis remains unknown—does its depletion trigger an irreversible commitment to sexual development, or are additional regulatory factors required to drive complete differentiation? The additive effects of a sexual differentiation-permissive environment, as generated in this study, suggest the latter. The *in vitro* approaches developed in this study provide valuable systems to address these questions in the future as well as support the testing of hypotheses pertaining to host-parasite co-evolution, chromatin regulation, and developmental plasticity, to further define the molecular events governing sexual commitment in *T. gondii*.

T. gondii infections have been widely reproduced *in vitro* using different cellular types and different cellular complexity from 2D to 3D systems. Vero and HFF are the most frequently used host cells to study diverse aspects of *in vitro T. gondii* biology.[40] In contrast, more complex systems—such as organoids and organ-on-a-chip models—have begun to illuminate how host architecture, cell diversity, and polarity influence parasite development. An instructive parallel comes from the related apicomplexan *Cryptosporidium*, whose entire life cycle was successfully reconstructed in intestinal organoids.[41] These advances suggest that stage transitions in apicomplexans can be experimentally recapitulated *in vitro* under appropriate architectural and metabolic conditions—highlighting the importance of using context-appropriate host models.

However, the widespread adoption of 3D intestinal organoids remains limited in part due to technical challenges, including microinjection requirements.[42] The success of intestinal monolayers derived from organoids further underscores the importance of epithelial polarity, cell type diversity, and apical accessibility. Unlike closed 3D structures, 2D monolayers expose the apical surface, closely mimicking the *in vivo* environment encountered during oral infection.[43] In our hands, these cultures supported not only bradyzoite formation but also the induction of pre-sexual and sexual forms, under FELIX and MORC depletion, suggesting that both cell types and culture structure influence the developmental outcome of *T. gondii* infections.

Moreover, recent work using human intestinal micro-physiological systems has demonstrated that *T. gondii* bradyzoites transmigrate the intestinal barrier and transition into tachyzoites upon reaching deeper tissues,[44] emphasizing the active role of intestinal epithelium in shaping infection dynamics. Our data extend this view by suggesting that epithelial context may also dictate the direction of differentiation, not just dissemination.

Given that both hRPE and organoid-derived monolayer-based models successfully support *T. gondii* differentiation, future studies comparing the transcriptional and metabolic landscape with that of other relevant models, such as human and feline intestinal models as well as feline intestinal epithelia, could provide deeper insights into host-specific factors that determine whether a parasite undergoes reactivation, encystation, dissemination, or sexual commitment.

This study establishes a tractable system for studying *T. gondii* sexual differentiation *in vitro*, opening new avenues for investigating the molecular mechanisms underlying this critical transition. A major goal for future research will be to determine whether parasites differentiated in this system can progress beyond early gametocyte stages to complete fertilization and oocyst formation. Achieving full gametogenesis *in vitro* would be a major breakthrough, enabling researchers to dissect late-stage sexual development without the need for feline hosts, abiding by the replacement principles in research (part of the 3Rs [reduce, reuse, recycle]).[45]

Ultimately, by modulating the key regulators of *T. gondii* sexual differentiation and leveraging host metabolic cues to manipulate its life cycle, this research brings us one step closer to developing targeted strategies to disrupt the parasite's transmission cycle. The insights gained from this model may also have broader implications for understanding life cycle regulation in related apicomplexan parasites, many of which depend on host-specific metabolic environments to complete their development.

Limitations of the study

A key limitation of 3D organoid models is the restricted access to the apical surface, which remains enclosed within the organoid lumen. This structural constraint hinders the study of pathogens that initiate infection from the intestinal lumen, such as *T. gondii*.[46] To overcome this barrier, we developed and optimized a monolayer system derived from murine intestinal organoids. Although this approach allows direct access to the apical surface and supports the formation of a confluent epithelial layer while retaining the expression of key intestinal cell markers, it does not fully reproduce the architectural complexity and spatial organization of the 3D model and the native intestinal tissue.[47] To overcome the limitation of restricted access to the luminal surface in conventional organoid models, the polarity inversion strategy (apical-out organoids), as described by Co et al. (2019),[48] offers a valuable alternative by exposing the apical domain to the culture medium—enabling direct interaction with luminal pathogens such as *T. gondii*.

A caveat of our study is that we initiated infections from tissue culture tachyzoites. The most widely accepted paradigm establishes that natural transitions into sexual stages may initiate from the bradyzoite stage. Therefore, initiating from tissue culture or mouse brain-derived bradyzoites might yield different results.

Another limitation is the difficulty in visualizing the terminal structures of the sexual stages of *T. gondii* within *in vitro* systems. However, we argue that this challenge reflects a broader issue in the field, namely the lack of standardized and validated reagents (such as stage-specific antibodies or reporters) and the limited availability of reliable indicator strains[21,49] rather than a limitation intrinsic to the model itself.

Finally, differences in the infection time points used between ODM and hRPE cell models represent a potential confounding factor when comparing sexual differentiation outcomes. These differences were primarily driven by the intrinsic constraints of each culture system, particularly the shorter viability window of the ODM cultures under the current experimental conditions, which restricts the long-term infection protocol.[50,51]

Nevertheless, recent developments are likely to improve the long-term maintenance of organoid systems. Particularly relevant to our work are the findings of Hryckowian and colleagues[28] who reported that feline intestinal organoids can be sustained more effectively by co-culturing them with fibroblasts, which, in turn, enable the recovery of merozoites. Combining such strategies with our approach could yield optimal output of sexual forms, thereby extending infection timelines and providing a more faithful mimic of the dynamics in natural host tissues.

In sum, breakthrough work established that host metabolic signals play a pivotal role in regulating *T. gondii* sexual differentiation. In parallel, the transcriptional repressor MORC was demonstrated to function as the molecular switch controlling the parasite's commitment to sexual development. By integrating these insights into a physiologically relevant *in vitro* model, we establish a foundation for further exploration of *T. gondii*'s differentiation and potential transmission-blocking strategies. Future research aimed at refining this system should focus on achieving full gametogenesis, opening new avenues to explore metabolic and genetic interventions that could disrupt the parasite's life cycle.

RESOURCE AVAILABILITY

Lead contact

Requests for further information and resources should be directed to and will be fulfilled by the lead contact, Maria E. Francia (mfrancia@pasteur.edu.uy).

Materials availability

This study did not generate new, unique reagents.

Data and code availability

- All data reported in this paper will be shared by the lead contact upon request.
- This paper does not report original code.
- Any additional information required to reanalyze the data reported in this paper is available from the lead contact upon request.

ACKNOWLEDGMENTS

We are deeply grateful to Dr. Mohamed-Ali Hakimi, University Grenoble Alpes, for sharing the *T. gondii* strain and reagents foundational to this work. We acknowledge the Advanced Bioimaging Unit at the Institut Pasteur Montevideo for their technical support and assistance with the microscopy facility platform. We thank our funding agencies. This project was funded by a G4 grant awarded to M.E.F. by the Pasteur Network; by ANII_FMV_1_2019_1_156213 to M.B.-F.; and FOCEM (MERCOSUR Structural Convergence Fund) and COF 03/1 to the IPM. S.C. received fellowships from Sistema Nacional de Becas (ANII) and Comisión Académica de Posgrado (CAP). F.S., M.E.F., M.C., M. B.-F., and R.P. are members of the SNI (National Research System, Uruguay) and researchers of PEDECIBA, Uruguay.

AUTHOR CONTRIBUTIONS

Conceptualization, M.E.F., R.P., M.C., and M.B.-F.; methodology, S.C. and F. S.; investigation, S.C. and F.S.; writing – original draft, all authors; writing – review & editing, all authors; funding acquisition, M.E.F., M.C., and M.B.-F.; and supervision, R.P., M.E.F., M.C., and M.B.-F.

DECLARATION OF INTERESTS

The authors declare no competing interests.

DECLARATION OF GENERATIVE AI AND AI-ASSISTED TECHNOLOGIES IN THE WRITING PROCESS

During the preparation of this work, no AI-assisted technologies were used.

STAR★METHODS

Detailed methods are provided in the online version of this paper and include the following:

- KEY RESOURCES TABLE
- EXPERIMENTAL MODEL AND STUDY PARTICIPANT DETAILS
  - Animals
  - Microbe strains
  - Cell lines
- METHOD DETAILS
  - Generation and maintenance of intestinal organoids (IOS)
  - Establishment of intestinal organoid-derived monolayers (ODM)
  - Cell viability determination of felix-treated organoids
  - Cell line infections
  - 2D and 3D murine intestinal organoid infections
  - 3D intestinal organoid inmunofluorescence assays
  - Felix-treated cell lines and intestinal organoid-derived monolayers inmunofluorescence assays
  - RNA isolation, cDNA synthesis, and qPCR
  - Confocal microscopy and imaging processing
- QUANTIFICATION AND STATISTICAL ANALYSIS

SUPPLEMENTAL INFORMATION

Supplemental information can be found online at https://doi.org/10.1016/j.celrep.2025.116451.

Received: April 30, 2025
Revised: September 4, 2025
Accepted: September 29, 2025
Published: October 17, 2025

REFERENCES

1. Dorsch, M.A., Francia, M.E., Tana, L.R., González, F.C., Cabrera, A., Calleros, L., Sanguinetti, M., Barcellos, M., Zarantonelli, L., Ciuffo, C., et al. (2022). Diagnostic Investigation of 100 Cases of Abortion in Sheep in Uruguay: 2015–2021. Front. Vet. Sci. *9*, 904786. https://doi.org/10.3389/fvets.2022.904786.
2. Halonen, S.K., and Weiss, L.M. (2013). Toxoplasmosis. Handb. Clin. Neurol. *114*, 125–145. https://doi.org/10.1016/B978-0-444-53490-3.00008-X.
3. Montoya, J.G., and Liesenfeld, O. (2004). Toxoplasmosis. Lancet *363*, 1965–1976. https://doi.org/10.1016/S0140-6736(04)16412-X.
4. Flegr, J., Prandota, J., Sovičková, M., and Israili, Z.H. (2014). Toxoplasmosis - A global threat. Correlation of latent toxoplasmosis with specific disease burden in a set of 88 countries. PLoS One. https://doi.org/10.1371/journal.pone.0090203.
5. Sibley, L.D., Khan, A., Ajioka, J.W., and Rosenthal, B.M. (2009). Genetic diversity of Toxoplasma gondii in animals and humans. Philos. Trans. R. Soc. Lond. B Biol. Sci. *364*, 2749–2761. https://doi.org/10.1098/rstb.2009.0087.
6. Torrey, E.F., and Yolken, R.H. (2013). Toxoplasma oocysts as a public health problem. Trends Parasitol. *29*, 380–384. https://doi.org/10.1016/j.pt.2013.06.001.
7. Pereira De Martinis, E.C., Alves, V.F., Pereira, M.G., Andrade, L.N., Abichabki, N., Abramova, A., Dannborg, M., and Bengtsson-Palme, J. (2025). Applying 3D cultures and high-throughput technologies to study host-pathogen interactions. Front. Immunol. *16*, 1–16. https://doi.org/10.3389/fimmu.2025.1488699.
8. Derricott, H., Luu, L., Fong, W.Y., Hartley, C.S., Johnston, L.J., Armstrong, S.D., Randle, N., Duckworth, C.A., Campbell, B.J., Wastling, J.M., and Coombes, J.L. (2019). Developing a 3D intestinal epithelium model for livestock species. Cell Tissue Res. *375*, 409–424. https://doi.org/10.1007/s00441-018-2924-9.
9. Luu, L., Johnston, L.J., Derricott, H., Armstrong, S.D., Randle, N., Hartley, C.S., Duckworth, C.A., Campbell, B.J., Wastling, J.M., and Coombes, J.L. (2019). An open-format enteroid culture system for interrogation of interactions between Toxoplasma gondii and the intestinal epithelium. Front. Cell. Infect. Microbiol. *9*, 300. https://doi.org/10.3389/fcimb.2019.00300.
10. Holthaus, D., Delgado-Betancourt, E., Aebischer, T., Seeber, F., and Klotz, C. (2020). Harmonization of protocols for multi-species organoid platforms to study the intestinal biology of Toxoplasma gondii and other protozoan infections. Front. Cell. Infect. Microbiol. *10*, 610368. https://doi.org/10.3389/fcimb.2020.610368.
11. Humayun, M., Ayuso, J.M., Park, K.Y., Martorelli Di Genova, B., Skala, M. C., Kerr, S.C., Knoll, L.J., and Beebe, D.J. (2022). Innate immune cell response to host-parasite interaction in a human intestinal tissue microphysiological system. Sci. Adv. *8*, eabm8012–eabm8018. https://doi.org/10.1126/sciadv.abm8012.
12. Sena, F., Cancela, S., Bollati-Fogolín, M., Pagotto, R., and Francia, M.E. (2023). Exploring Toxoplasma gondiís Biology within the Intestinal Epithelium: intestinal-derived models to unravel sexual differentiation. Front. Cell. Infect. Microbiol. *13*. https://doi.org/10.3389/fcimb.2023.1134471.
13. Frenkel, J.K., and Dubey, J.P. (1972). Toxoplasmosis and its prevention in cats and man. J. Infect. Dis. *126*, 664–673.
14. Pelster, B., and Piekarski, G. (1971). Elektronenmikroskopische Analyse der Mikrogametenentwicklung bei Toxoplasma gondii. Z. Parasitenkd. *37*, 267–277. https://doi.org/10.1007/BF00259333.
15. Ferguson, D.J., Hutchison, W.M., and Siim, J.C. (1975). the Ultrastructural Development of the Macrogamete and Formation of the Oocyst Wall of Toxoplasma Gondii. Acta Pathol. Microbiol. Scand. B *83*, 491–505. https://doi.org/10.1111/j.1699-0463.1975.tb00130.x.
16. Martorelli Di Genova, B., and Knoll, L.J. (2020). Comparisons of the Sexual Cycles for the Coccidian Parasites Eimeria and Toxoplasma. Front. Cell. Infect. Microbiol. *10*, 604897. https://doi.org/10.3389/fcimb.2020.604897.
17. Farhat, D.C., Swale, C., Dard, C., Cannella, D., Ortet, P., Barakat, M., Sindikubwabo, F., Belmudes, L., De Bock, P.J., Couté, Y., et al. (2020). A MORC-driven transcriptional switch controls Toxoplasma developmental trajectories and sexual commitment. Nat. Microbiol. *5*, 570–583. https://doi.org/10.1038/s41564-020-0674-4.

18. Gross, U., Bormuth, H., Gaissmaier, C., Dittrich, C., Krenn, V., Bohne, W., and Ferguson, D.J. (1995). Monoclonal rat antibodies directed against toxoplasma gondii suitable for studying tachyzoite-bradyzoite interconversion in vivo. Clin. Diagn. Lab. Immunol. *2*, 542–548. https://doi.org/10.1128/cdli.2.5.542-548.1995.
19. Antunes, A.V., Shahinas, M., Swale, C., Farhat, D.C., Ramakrishnan, C., Bruley, C., Cannella, D., Robert, M.G., Corrao, C., Couté, Y., et al. (2024). In vitro production of cat-restricted Toxoplasma pre-sexual stages. Nature *625*, 366–376. https://doi.org/10.1038/s41586-023-06821-y.
20. Scholtyseck, E., Mehlhorn, H., and Hammond, D.M. (1972). Electron microscope studies of microgametogenesis in coccidia and related groups. Z. Parasitenkd. *38*, 95–131.
21. Di Genova, B.M., Wilson, S.K., Dubey, J.P., and Knoll, L.J. (2019). Intestinal delta-6-desaturase activity determines host range for Toxoplasma sexual reproduction. PLoS Biol. *17*, 1–19. https://doi.org/10.1371/journal.pbio.3000364.
22. Fan, F., Xue, L., Yin, X., Gupta, N., and Shen, B. (2023). AP2XII-1 is a negative regulator of merogony and presexual commitment in Toxoplasma gondii. mBio *14*, e0178523. https://doi.org/10.1128/mbio.01785-23.
23. Srivastava, S., Holmes, M.J., White, M.W., and Sullivan, W.J. (2023). Toxoplasma gondii AP2XII-2 Contributes to Transcriptional Repression for Sexual Commitment. mSphere *8*, e0060622. https://doi.org/10.1128/msphere.00606-22.
24. Wang, J.L., Li, T.T., Zhang, N.Z., Wang, M., Sun, L.X., Zhang, Z.W., Fu, B. Q., Elsheikha, H.M., and Zhu, X.Q. (2024). The transcription factor AP2XI-2 is a key negative regulator of Toxoplasma gondii merogony. Nat. Commun. *15*, 793. https://doi.org/10.1038/s41467-024-44967-z.
25. Jiang, Y., Shi, Y., Xue, Y., Hu, D., and Song, X. (2024). AP2XII-1 and AP2XI-2 Suppress Schizogony Gene Expression in Toxoplasma gondii. Int. J. Mol. Sci. *25*, 5527. https://doi.org/10.3390/ijms25105527.
26. Rivers, J.P., Sinclair, A.J., and Craqford, M.A. (1975). Inability of the cat to desaturate essential fatty acids. Nature *258*, 171–173. https://doi.org/10.1038/258171a0.
27. Sinclair, A.J., McLean, J.G., and Monger, E.A. (1979). Metabolism of linoleic acid in the cat. Lipids *14*, 932–936. https://doi.org/10.1007/BF02533508.
28. Hryckowian, N.D., Ramírez-Flores, C.J., Zinda, C., Park, S.C., Kelty, M.T., and Knoll, L.J. (2024). Host cell-specific metabolism of linoleic acid controls Toxoplasma gondii growth in cell culture. Infect. Immun. *92*, 1–18. https://doi.org/10.1128/iai.00299-24.
29. Hurst, R.J.M., and Else, K.J. (2012). Retinoic acid signalling in gastrointestinal parasite infections: Lessons from mouse models. Parasite Immunol. *34*, 351–359. https://doi.org/10.1111/j.1365-3024.2012.01364.x.
30. Smith, J.R., Ashander, L.M., Arruda, S.L., Cordeiro, C.A., Lie, S., Rochet, E., Belfort, R., and Furtado, J.M. (2021). Pathogenesis of ocular toxoplasmosis. Prog. Retin. Eye Res. *81*, 100882. https://doi.org/10.1016/j.preteyeres.2020.100882.
31. Smith, J.R., Ashander, L.M., Ma, Y., Rochet, E., and Furtado, J.M. (2020). Model Systems for Studying Mechanisms of Ocular Toxoplasmosis. In Toxoplasma Gondii. Methods in Molecular Biology, O.S. Harb, D.S. Roos, and C.J. Tonkin, eds. (Springer Nature), pp. 297–321. https://doi.org/10.1007/978-1-4939-9857-9_17.
32. Nogueira, A.R., Leve, F., Morgado-Diaz, J., Tedesco, R.C., and Pereira, M. C.S. (2016). Effect of Toxoplasma gondii infection on the junctional complex of retinal pigment epithelial cells. Parasitology *143*, 568–575. https://doi.org/10.1017/S0031182015001973.
33. Furtado, J.M., Bharadwaj, A.S., Chipps, T.J., Pan, Y., Ashander, L.M., and Smith, J.R. (2012). Toxoplasma gondii tachyzoites cross retinal endothelium assisted by intercellular adhesion molecule-1 in vitro. Immunol. Cell Biol. *90*, 912–915. https://doi.org/10.1038/icb.2012.21.
34. Furtado, J.M., Ashander, L.M., Mohs, K., Chipps, T.J., Appukuttan, B., and Smith, J.R. (2013). Toxoplasma gondii Migration within and Infection of Human Retina. PLoS One *8*, e54358. https://doi.org/10.1371/journal.pone.0054358.
35. Lie, S., Vieira, B.R., Arruda, S., Simões, M., Ashander, L.M., Furtado, J.M., and Smith, J.R. (2019). Molecular basis of the retinal pigment epithelial changes that characterize the ocular lesion in toxoplasmosis. Microorganisms *7*, 405. https://doi.org/10.3390/microorganisms7100405.
36. Ashander, L.M., Lie, S., Ma, Y., Rochet, E., Washington, J.M., Furtado, J. M., Appukuttan, B., and Smith, J.R. (2019). Neutrophil activities in human ocular toxoplasmosis: An in vitro study with human cells. Investig. Ophthalmol. Vis. Sci. *60*, 4652–4660. https://doi.org/10.1167/iovs.19-28306.
37. Smith, D., Price, D.R.G., Burrells, A., Faber, M.N., Hildersley, K.A., Chintoan-Uta, C., Chapuis, A.F., Stevens, M., Stevenson, K., Burgess, S.T.G., et al. (2021). The development of ovine gastric and intestinal organoids for studying ruminant host-pathogen interactions. Front. Cell. Infect. Microbiol. *11*, 733811–733818. https://doi.org/10.3389/fcimb.2021.733811.
38. Ashander, L.M., Lidgerwood, G.E., Lumsden, A.L., Furtado, J.M., Pébay, A., and Smith, J.R. (2025). Human Retinal Organoid Model of Ocular Toxoplasmosis. Pathogens *14*, 286. https://doi.org/10.3390/pathogens14030286.
39. Dubey, J.P., Lindsay, D.S., and Speer, C.A. (1998). Structures of Toxoplasma gondii tachyzoites, bradyzoites, and sporozoites and biology and development of tissue cysts. Clin. Microbiol. Rev. *11*, 267–299.
40. Khan, A., and Grigg, M.E. (2017). Toxoplasma gondii: Laboratory maintenance and growth. Curr. Protoc. Microbiol. *44*, 20C.1.1–20C.1.17. https://doi.org/10.1002/cpmc.26.Toxoplasma.
41. Heo, I., Dutta, D., Schaefer, D.A., Iakobachvili, N., Artegiani, B., Sachs, N., Boonekamp, K.E., Bowden, G., Hendrickx, A.P.A., Willems, R.J.L., et al. (2018). Modelling Cryptosporidium infection in human small intestinal and lung organoids. Nat. Microbiol. *3*, 814–823. https://doi.org/10.1038/s41564-018-0177-8.
42. Wilson, S.S., Mayo, M., Melim, T., Knight, H., Patnaude, L., Wu, X., Phillips, L., Westmoreland, S., Dunstan, R., Fiebiger, E., and Terrillon, S. (2020). Optimized Culture Conditions for Improved Growth and Functional Differentiation of Mouse and Human Colon Organoids. Front. Immunol. *11*, 547102–547118. https://doi.org/10.3389/fimmu.2020.547102.
43. Forbester, J.L., Goulding, D., Vallier, L., Hannan, N., Hale, C., Pickard, D., Mukhopadhyay, S., and Dougan, G. (2015). Interaction of salmonella enterica serovar Typhimurium with intestinal organoids derived from human induced pluripotent stem cells. Infect. Immun. *83*, 2926–2934. https://doi.org/10.1128/IAI.00161-15.
44. Ramírez-Flores, C.J., Hryckowian, N.D., Gale, A.N., Babatunde, K.A., Lares, M., Beebe, D.J., Kerr, S.C., and Knoll, L.J. (2025). Modeling Toxoplasma gondii-gut early interactions using a human microphysiological system. PLoS Negl. Trop. Dis. *19*, e0012855. https://doi.org/10.1371/journal.pntd.0012855.
45. Russell, W. (2005). The Three Rs: past, present and future. Anim. Welf. *14*, 279–286. https://doi.org/10.1017/S0962728600029596.
46. Ferguson, D.J.P. (2004). Use of molecular and ultrastructural markers to evaluate stage conversion of Toxoplasma gondii in both the intermediate and definitive host. Int. J. Parasitol. *34*, 347–360. https://doi.org/10.1016/j.ijpara.2003.11.024.
47. Sato, T., Vries, R.G., Snippert, H.J., Van De Wetering, M., Barker, N., Stange, D.E., Van Es, J.H., Abo, A., Kujala, P., Peters, P.J., and Clevers, H. (2009). Single Lgr5 stem cells build crypt-villus structures in vitro without a mesenchymal niche. Nature *459*, 262–265. https://doi.org/10.1038/nature07935.
48. Co, J.Y., Margalef-Català, M., Li, X., Mah, A.T., Kuo, C.J., Monack, D.M., and Amieva, M.R. (2019). Controlling Epithelial Polarity: A Human Enteroid Model for Host-Pathogen Interactions. Cell Rep. *26*, 2509–2520.e4. https://doi.org/10.1016/j.celrep.2019.01.108.

49. Ramakrishnan, C., Maier, S., Walker, R.A., Rehrauer, H., Joekel, D.E., Winiger, R.R., Basso, W.U., Grigg, M.E., Hehl, A.B., Deplazes, P., and Smith, N.C. (2019). An experimental genetically attenuated live vaccine to prevent transmission of Toxoplasma gondii by cats. Sci. Rep. *9*, 1474. https://doi.org/10.1038/s41598-018-37671-8.

50. Warschkau, D., and Seeber, F. (2023). Advances towards the complete in vitro life cycle of Toxoplasma gondii. Fac. Rev. *12*, 1. https://doi.org/10.12703/r/12-1.

51. Kozuka, K., He, Y., Koo-McCoy, S., Kumaraswamy, P., Nie, B., Shaw, K., Chan, P., Leadbetter, M., He, L., Lewis, J.G., et al. (2017). Development and Characterization of a Human and Mouse Intestinal Epithelial Cell Monolayer Platform. Stem Cell Rep. *9*, 1976–1990. https://doi.org/10.1016/j.stemcr.2017.10.013.

52. Harning, D., Spenter, J., Metsis, A., Vuust, J., and Petersen, E. (1996). Recombinant Toxoplasma gondii surface antigen 1 (P30) expressed in Escherichia coli is recognized by human Toxoplasma-specific immunoglobulin M (IgM) and IgG antibodies. Clin. Diagn. Lab. Immunol. *3*, 355–357. https://doi.org/10.1128/cdli.3.3.355-357.1996.

53. Ramakrishnan, C., Maier, S., Walker, R.A., Rehrauer, H., Joekel, D.E., Winiger, R.R., Basso, W.U., Grigg, M.E., Hehl, A.B., Deplazes, P., and Smith, N.C. (2019). An experimental genetically attenuated live vaccine to prevent transmission of Toxoplasma gondii by cats. Sci. Rep. *9*, 1–14. https://doi.org/10.1038/s41598-018-37671-8.

54. Bogado, S., Dalmasso, M.C., Ganuza, A., Kim, K., Sullivan, W.J., Jr., Angel, S.O., and Vanagas, L. (2014). Canonical histone H2Ba and H2A.X dimerize in an opposite genomic localization to H2A.Z/H2B.Z dimers in Toxoplasma gondii. Mol. Biochem. Parasitol. *197*, 36–42. https://doi.org/10.1016/j.molbiopara.2014.09.009.

55. Di Genova, B.M., Wilson, S.K., Dubey, J.P., and Knoll, L.J. (2019). Intestinal delta-6-desaturase activity determines host range for Toxoplasma sexual reproduction. PLoS Biol. *17*, 1–19. https://doi.org/10.1371/journal.pbio.3000364.

56. Daghero, H., Doffe, F., Varela, B., Yozzi, V., Verdes, J.M., Crispo, M., Bollati-Fogolín, M., and Pagotto, R. (2022). Jejunum-derived NF-κB reporter organoids as 3D models for the study of TNF-alpha-induced inflammation. Sci. Rep. *12*, 14425. https://doi.org/10.1038/s41598-022-18556-3.

STAR★METHODS

KEY RESOURCES TABLE

REAGENT or RESOURCE	SOURCE	IDENTIFIER
Antibodies		
anti-Sag1	Kindly provided by Dr. Dominique Soldati, Université de Genève	Harning et al.[52]
anti-cc2	Kindly provided by Dr. Dominique Soldati, Université de Genève	Gross et al.[18]
anti-GRA11b	Kindly provided by Dr. Chandra Ramakrishnan, University of Zurich	Ramakrishnan et al.[53]
anti-h2bz	Kindly provided by Laura Vanagas, INTECH-Chascomus	Bogado et al.[54]
anti-AO2	Kindly provided by Dr. Chandra Ramakrishnan, University of Zurich	Di Genova, et al.[55]
Goat anti-rat IgG Alexa Fluor 488	Invitrogen	A11006; RRID: AB_2534074
Goat anti-mouse IgG Alexa Fluor 488	Invitrogen	A28175; RRID: AB_2536161
Goat anti-rabbit IgG Alexa Fluor 488	Invitrogen	A11008; RRID: AB_143165
Goat anti-rabbit IgG Alexa Fluor 594	Invitrogen	A11012; RRID: AB_2534079
Experimental models: Cell lines		
Vero cells	ATCC	CCL-81
hTERT RPE	ATCC	CRL-4000
Caco-2	ATCC	HTB-37
NSC-34	Kindly provided by Dr. Luis Barbeito (Institut Pasteur de Montevideo)	N/A
Experimental models: Organisms/strains		
Mus musculus	Laboratory Animal Biotechnology Unit of the Institut Pasteur	C57BL/6J
Toxoplasma gondii	Kindly provided by Dr. Mohamed-Ali Hakimi, University of Grenoble (Farhat et al.[17])	PruΔku80 MORC–mAID–Tir-HA
Toxoplasma gondii		PruΔku80
Oligonucleotides		
TUBA1 (TGME49_116400)	IDT	F: GACGACGCCTTCAACACCTTCTTT R: AGTTGTTCGCAGCATCCTCTTTC
SAG1 (TGME49_233460)	IDT	F: AGCATTTCCAGCCGAGTCAA R: TGCACGGTACAGTGATGCTT
BAG1 (TGME49_259020)	IDT	F: GATGACGTAACCATAGAAGTCG ACAAC R: GCAAAATAACCGGACA CTCGCTCAGTC
GRA81 (TGME49_243940)	IDT	F: CTCGAAAACCCGAACATCGC R: CCCTTCCAAGCTGGACAAGT
GRA11b (TGME49_237800)	IDT	F: ATCAAGTCGCACGAGACGCC R: AGCGAATTGCGTTCCCTGCT
PF16 (TGME49_297820)	IDT	F: CACACCTAGCTGCCTTGGAA R: GGCAAAACCTTGGCGTACTG
IFT122 (TGME49_218290)	IDT	F: GCAAAAGCGTTCACACGACT R: TGCGCTGTCGAAGAAGAGTT
AO2 (TGME49_286778)	IDT	F: GACCGTTATATCCGTGACAACGAG R:TATGCCAAACAGAGGACGCAAC
Software and algorithms		
Fiji		N/A

(*Continued on next page*)

Continued		
REAGENT or RESOURCE	SOURCE	IDENTIFIER
GraphPad Prism	GraphPad Software, Boston, Massachusetts USA, www.graphpad.com	version 10.0.0 for Mac
Other		
Phalloidin- Texas Red	Invitrogen	T7471
DAPI	Thermo	62248
Lysozyme	DAKO- Santa Clara	A0099

EXPERIMENTAL MODEL AND STUDY PARTICIPANT DETAILS

Animals

6-8 weeks old, male and female *Mus musculus* C57BL/6J were used to establish organoid cultures as described below. Animals were maintained *in house* following protocols pre-approved by the Institutional Comisión de Ética en el Uso de Animales (CEUA) (protocol N° 002–21) and were performed abiding by the national law of animal experimentation (#18.611), established according to relevant international laboratory animal welfare guidelines and regulations. Animals were bred in house at the animal housing facility of Institut Pasteur de Montevideo, and maintained herein in controlled light and temperature conditions. A maximum of six animals were housed per cage and food and water were provided *ad libitum*. Bedding and environmental enrichment props were changed weekly. C57BL/6J mice were bred at the Laboratory Animal Biotechnology Unit of the Institut Pasteur de Montevideo under specific pathogen-free conditions in ventilated racks (IVC, 1285L, Tecniplast, Milan, Italy). Animals were euthanized with CO2 followed by cervical dislocation, and intestine biopsies were immediately removed.

Microbe strains

Toxoplasma gondii PruΔku80 MORC–mAID–Tir-HA and PruΔku80 used in this work were kindly provided by Dr. Mohamed-Ali Hakimi, University of Grenoble Alpes.[17] Parasites were maintained in kidney cells derived from an african green monkey (Vero cells; ATCC CCL-81). Cultures routinely tested negative for presence of mycoplasma.

Cell lines

Vero cells; (ATCC CCL-81), human retinal pigmented epithelial (hTERT RPE1, so called hRPE; ATCC CRL-4000), human colorectal adenocarcinoma (Caco-2; ATCC HTB-37), and murine motor neuron-like cells (NSC-34; kindly provided by Dr. Luis Barbeito, Institut Pasteur de Montevideo) were maintained in Dulbecco’s Modified Eagle medium (DMEM, Gibco) supplemented with 10% (v/v) fetal bovine serum (Gibco), 4 mM L-glutamine (Gibco), 200 U/mL of penicillin, 200 mg/mL of streptomycin (Gibco), unless otherwise specified. Cultures routinely tested negative for presence of mycoplasma.

METHOD DETAILS

Generation and maintenance of intestinal organoids (IOS)

Murine small intestine tissue from C57BL/6J mice (6–8 weeks old, male and female) were collected by dissection. The small intestine was cut into 5 cm-long tissue sections and flushed out with ice-cold sterile phosphate-buffered saline (PBS) supplemented with 1% (w/v) penicillin/streptomycin to remove luminal contents. The tissues were sliced longitudinally, cut into 0.5 cm fragments, and washed in cold PBS until the supernatant was clear. Following a 20 min incubation in 10 mM ethylenediaminetetraacetic acid (EDTA) in PBS with gentle agitation, EDTA was removed, and the fragments were resuspended in 0.1% (w/v) bovine serum albumin (BSA) in PBS. The suspension was pipetted up and down five times with a 10 mL pipette to ensure crypt release.[56]

Crypt-enriched fractions were pooled and filtered using a 70 μm cell strainer. The isolated crypts were then centrifuged at 200 g for 5 min at 4°C, counted, and resuspended in phenol red-free, growth factors-reduced basement membrane extract (Matrigel , Corning) at a density of 300 crypts/20 μL matrix. Crypt/matrix droplets were seeded in a 6 well plate and incubated at 37°C for 10 min to allow matrix polymerization. Subsequently, 2 mL per well of organoid medium (Advanced DMEM/F12 (Gibco), 1% (w/v) L-glutamine, 1% (w/v) penicillin/streptomycin, 50% (v/v) L-WRN conditioned medium) supplemented with 10 μM Y-27632 (ROCK inhibitor, PeproTech), and 10 μM SB431542 (TGF-β inhibitor, PeproTech) was added. The L-WRN media was produced in our laboratory by the commercially available cell line L-WRN (ATCC 3276) as previously described (Daghero et al., 2022). Organoids were incubated at 37°C in a 5% CO2 humidified atmosphere.

For maintenance, the medium was renewed every 2–3 days with organoid medium without inhibitors. Organoids were subcultured every 4–5 days at a 1:2 or 1:3 ratio using organoid medium supplemented with ROCK and TGF-β inhibitors, and used at passages 3–8. Model characterization is provided in Figure S1, according to Daghero, 2022.[56]

Establishment of intestinal organoid-derived monolayers (ODM)

To form monolayers from intestinal organoids, full-grown 3D organoids were used at day three of culture for plating in 24 multi-well plates. Plates were pre-coated with 120 μL per well of a 1:10 Matrigel -PBS solution and incubated for at least 1 h at 37°C. Organoids were recovered from matrix domes using ice-cold PBS and washed twice at 200 g for 5 min at 4°C. Organoids were resuspended in TrypLE Express 1 × (Gibco) supplemented with 10 mM Y-27632 and incubated at 37°C for 4 min. To facilitate cell disaggregation, the suspension was shaken every 2 min. After TrypLE inactivation with organoid medium, cells were mechanically dissociated until single cell suspension. Then, cells were counted and seeded in the pre-coated plate (2 × 105 cells/well). For the ODM-specific medium, organoid medium was supplemented with 10 μM Y-27632 (PeproTech), 10 μM SB431542 (PeproTech), 2.5 μM CHIR99021 (GSK-3 inhibitor) (PeproTech), 10 μM SB202190 (Sigma-Aldrich), 1 mM N-acetyl cysteine (Sigma- Aldrich) and 10 mM Nicotinamide (Sigma-Aldrich), and renewed every two days until cells reach 80% confluency. Intestinal monolayers characterization is provided in Figure S2, according to Daghero, 2023.

Cell viability determination of felix-treated organoids

To assess the cytotoxicity of compounds used to generate FELIX, 3D and 2D intestinal organoids were cultured under standard conditions before treatment. On day 2 of culture, the medium was replaced with FELIX media: fresh complete culture medium containing free form of linoleic acid (200 μM) (Sigma, #62240) and the delta-6-desaturase inhibitor SC-26196 (20 μM) to emulate the feline intestinal environment. The treatment medium was refreshed every two days, and cell viability was evaluated at days 2, 3, and 5 post-treatments using the 3-(4,5-Dimethylthiazol-2-yl)-2,5-Diphenyltetrazolium Bromide (MTT) assay. For the assay, 10 μL of a 5 mg/mL MTT solution (SIGMA, M5655) was added to each well and incubated for 3 h at 37°C in a humidified 5% CO_2 atmosphere. After incubation, the medium was removed, and 20 μL of 20% (w/v) sodium dodecyl sulfate (SDS) was added to dissolve the extracellular matrix, followed by a 1-h incubation at 37°C. Subsequently, 100 μL of a 1:1 dimethyl sulfoxide (DMSO): isopropanol solution was added to solubilize the formazan crystals, and absorbance was measured at 570 nm. For data analysis, cell viability at each time point and condition (treated or untreated) was expressed as a percentage relative to the untreated control at day 3, which was set as 100%. This normalization strategy allowed us to monitor both the effects of treatment over time and the natural evolution of the cultures in the absence of treatment (Figure S3).

Cell line infections

The Vero, hRPE, Caco-2, and NSC-34 monolayers were grown to confluence and infected with 1 × 10^7 PruΔku80 MORC–mAID–Tir-HA tachyzoites under growth conditions described below. After 24 h of infection, the media was changed to induce parasite sexual differentiation. Differentiation was first induced by incubation in Roswell Park Memorial Institute 1640 medium (RPMI, Gibco), 1% fetal bovine serum, 20 U/mL of penicillin, 20 mg/mL of streptomycin, 10 μM *trans*-retinoic acid (Abcam 120728) at pH 8.2, and FELIX (linoleic acid (200 μM) (Sigma, 62240) and the delta-6-desaturase inhibitor SC-26196 (20 μM)). Cultures were incubated at 37°C in low CO2 conditions for seven days. The media was changed every other day. On day 5, 500 μM indoleacetic acid (IAA; Sigma I2886) was added to induce MORC depletion (referred to as "+IAA" throughout the manuscript), and cultures were grown for an additional 2 days, for a total of 7 days.

2D and 3D murine intestinal organoid infections

To evaluate *T. gondii* infection and differentiation in different host cell contexts, both three-dimensional (3D) and two-dimensional (2D) murine intestinal organoid cultures were used. A type II strain of moderate virulence (PruΔku80) was used for optimization experiments, and the transgenic strain PruΔku80 MORC–mAID–Tir-HA for parasite differentiation assays. Non-infected controls were included for both 2D and 3D setups using the corresponding culture conditions.

For the 3D organoid infections, the murine intestinal organoids were generated as described in below and maintained in organoid medium. On day 3, intact or partially dissociated 3D organoids—partially dissociated to expose the luminal (apical) surface while preserving epithelial architecture— were incubated in suspension with tachyzoites (PruΔku80 strain) at a MOI of 1:1 for 90 min at 37°C in a humidified atmosphere containing 5% CO_2. Following infection, organoids were washed with PBS 1× to remove extracellular parasites, centrifuged at 260 g for 5 min, embedded in fresh matrix droplets, and seeded in 24-well plates containing glass coverslips. After matrix polymerization (10 min, 37°C), 500 μL of organoid medium supplemented with ROCK and TGF-B inhibitors was added per well. Cultures were maintained for 24 h post-infection at 37°C and 5% CO_2 before being processed for immunofluorescence as described below.

For the 2D organoid-derived monolayer infections, the murine intestinal ODM were established on coated coverslips as described below and maintained in ODM-specific medium. On day 2, cultures were incubated in FELIX media by supplementing the medium with 200 μM linoleic acid and 20 μM delta-6-desaturase inhibitor (Sigma, SC-26196).

On days 3–4, both FELIX-treated and untreated monolayers were infected with tachyzoites. For optimization assays, the PruΔku80 strain was used at a MOI of 1:1 for 90 min at 37°C. For T gondii differentiation assays, the transgenic PruΔku80 MORC–mAID–Tir-HA strain was used at a MOI of 1:6 for 2 h at 37°C. Two hours post-infection, 500 μM indole-3-acetic acid was added to induce MORC degradation and promote *T. gondii*'s stage conversion (+IAA).

Cultures were maintained for 24 h (optimization) or 48 h (*T. gondii* differentiation) post-infection and then processed for RNA extraction and/or immunofluorescence assay, as described below.

3D intestinal organoid inmunofluorescence assays

Organoids were removed from the matrix using cold 1 × PBS and fixed in 4% paraformaldehyde (PFA) for 30–60 min at room temperature (RT), followed by two washes with cold 1 × PBS. Organoids were allowed to sediment or were centrifuged at low speed (180 g 5 min) to minimize disruption. Care was taken to avoid excessive pipetting, and tips and tubes were pre-coated with 0.1% (w/v) BSA to prevent adhesion of organoids to plastic surfaces.

Organoids were blocked in blocking buffer (2.5% (w/v) BSA in 1 × PBS) and incubated in permeabilization buffer (0.5% Triton X-100 in blocking buffer) for 2 h at RT. All antibodies were prepared in blocking buffer. Samples were incubated with primary antibodies overnight at 4°C. Following three washes in 1 × PBS (5 min each), samples were incubated with secondary antibodies and fluorescent dyes for 1 h at RT. After three additional 1 × PBS washes, organoids were mounted on glass-bottom plates in ProLong Gold Antifade Reagent (Invitrogen, P36930). Fluorescent dyes and antibodies used are listed in Table S1.

Felix-treated cell lines and intestinal organoid-derived monolayers inmunofluorescence assays

Host cells were grown to 90% confluency on 13 mm glass coverslips and infected with 107–108 extracellular parasites. Intracellular parasites were fixed at the time points indicated in the corresponding figures, using methanol for 5 min at −20°C or 4% PFA for 20 min at RT in ODM, followed by two washes with cold 1 × PBS. Cultures were blocked in blocking buffer 1 × PBS and 3% (w/v) BSA for 10 min or 1 h at RT, cell lines and ODM, respectively. Primary and secondary antibodies were prepared on 1× PBS and 3% (w/v) BSA and incubated at room temperature for 1h each. After the incubation of the secondary antibody, coverslips were three times washed with 1 × PBS for 10 min each and mounted onto ProLongTM Glass Antifade. Fluorescent dyes and antibodies used are listed in Table S1.

RNA isolation, cDNA synthesis, and qPCR

RNA was extracted using Direct-zol RNA Miniprep kit (Zymo Research, R2050) or Monarch total RNA miniprep kit (New England Biolabs, T2010S). First-strand cDNA was synthesized approximately 0.5–1 μg total RNA using SuperScript II Reverse Transcriptase (Invitrogen, 18064-022) or M-MLV Reverse Transcriptase (ThermoFisher Scientific, 28025013) and following the supplier's recommendations. qPCR reactions were conducted on each sample in triplicate, on a QuantStudio 3 System real-time PCR detection equipment using the FastStart Universal SYBR Green Master (Roche, 04 913 850 001). The PCR program used was: 10 min 95°C and 40 times (10 s at 95°C and 60 s at 60°C). All oligonucleotide sequences are listed in Table S2. Expression values for each gene were normalized to the reference alpha tubulin 1 gene (TGME49_116400) to obtain the Δct. Four different treatments were studied, (1) - FELIX -IAA, (2) - FELIX +IAA, (3) + FELIX -IAA, and (4) + FELIX +IAA. Finally, the relative expression of each gene of interest (GOI) was plotted as the mean of three biological replicates and it was obtained by the comparison of each treatment against the - FELIX and -IAA control condition. The relative expression represents 2-ΔΔct where ΔΔct is obtained as: ΔΔct (GOI) = Δct (GOI) treatment - Δct (GOI) control.

Confocal microscopy and imaging processing

IFAs were observed by confocal microscopy using either a Zeiss confocal LSM880 or LSM800 microscopes equipped with a Plan-Apochromat immersion oil 63 × lens with a numerical aperture of 1.40. All images were acquired and processed using the Zeiss ZEN blue edition v3.9 software. Image analysis was performed using Fiji.

QUANTIFICATION AND STATISTICAL ANALYSIS

Analysis of variance (two-way ANOVA) were performed with data from at least three replicates in all the cases. Means were compared using Tukey's post-hoc honest significant difference test with multiple comparisons at the $p < 0.05$ level using GraphPad Prism version 10.0.0 for Mac (GraphPad Software, Boston, Massachusetts USA, www.graphpad.com).